

# PROCEEDINGS OF SPIE

[SPIDigitalLibrary.org/conference-proceedings-of-spie](https://SPIDigitalLibrary.org/conference-proceedings-of-spie)

## High-aspect ratio zone plate fabrication for hard x-ray nanoimaging

Karolis Parfeniukas, Stylianos Giakoumidis, Rabia Akan,  
Ulrich Vogt

**SPIE.**

# High-aspect ratio zone plate fabrication for hard x-ray nanoimaging

Karolis Parfeniukas<sup>a\*</sup>, Stylianos Giakoumidis<sup>a</sup>, Rabia Akan<sup>a</sup>, and Ulrich Vogt<sup>a</sup>

<sup>a</sup>KTH Royal Institute of Technology, Biomedical and X-ray Physics, Albanova University Center, 10691 Stockholm, Sweden

## ABSTRACT

We present our results in fabricating Fresnel zone plate optics for the NanoMAX beamline at the fourth-generation synchrotron radiation facility MAX IV, to be used in the energy range of 6–10 keV. The results and challenges of tungsten nanofabrication are discussed, and an alternative approach using metal-assisted chemical etching (MACE) of silicon is showcased.

We successfully manufactured diffraction-limited zone plates in tungsten with 30 nm outermost zone width and an aspect ratio of 21:1. These optics were used for nanoimaging experiments at NanoMAX.

However, we found it challenging to further improve resolution and diffraction efficiency using tungsten. High efficiency is desirable to fully utilize the advantage of increased coherence on the optics at MAX IV. Therefore, we started to investigate MACE of silicon for the nanofabrication of high-resolution and high-efficiency zone plates.

The first type of structures we propose use the silicon directly as the phase-shifting material. We have achieved 6  $\mu\text{m}$  deep dense vertical structures with 100 nm linewidth.

The second type of optics use iridium as the phase material. The structures in the silicon substrate act as a mold for iridium coating via atomic layer deposition (ALD). A semi-dense pattern is used with line-to-space ratio of 1:3 for a so-called frequency-doubled zone plate. This way, it is possible to produce smaller structures with the tradeoff of the additional ALD step. We have fabricated 45 nm-wide and 3.6  $\mu\text{m}$ -tall silicon/iridium structures.

**Keywords:** zone plate, high-aspect ratio, etching, RIE, MACE, tungsten, silicon, gold

## 1. INTRODUCTION

High-resolution x-ray optics are of utmost importance for modern x-ray nanoimaging. High efficiency is also desirable to fully utilize the advantage of increased coherence at the optics at fourth generation synchrotron radiation facilities such as MAX IV. We present our findings while fabricating Fresnel zone plate optics for the NanoMAX beamline at MAX IV, to be used in the energy range of 6–10 keV.

## 2. TUNGSTEN-BASED ZONE PLATES

Fresnel zone plates for the hard x-ray regime require a dense material to act as the phase shifting medium.<sup>1</sup> Tungsten is suitable because of its high density and documented methods of deposition and etching. Another advantage is that the ability to deposit tungsten enables usage of x-ray transparent substrates, such as silicon nitride membranes.

This section describes a fabrication method of high resolution tungsten zone plates and related challenges, as well as the usage of our fabricated devices.

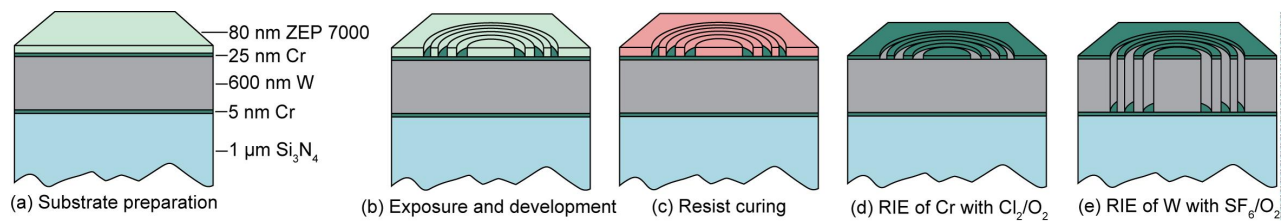


Figure 1. Fabrication process of tungsten zone plates. (a) Substrate preparation. (b) The zone plate pattern is written using electron beam lithography and then developed. (c) The remaining resist is cured with a large electron dose. (d) Using reactive ion etching, the pattern is transferred into chromium. (e) The pattern is etched into tungsten.

## 2.1 Fabrication

Figure 1 illustrates the fabrication process of tungsten zone plates, published earlier.<sup>2</sup> A material stack is prepared: 1  $\mu\text{m}$  silicon nitride, 5 nm chromium, 600 nm tungsten, 25 nm chromium, and 80 nm ZEP7000. The resist is baked at 170°C for 30 minutes in a convection oven. The pattern defining the zone plate structures is exposed using electron beam lithography. The resist is developed in -18°C hexylacetate. Then, the resist in the patterned area is cured with a 30 000  $\mu\text{C}/\text{cm}^2$  dose at 5 keV to improve pattern transfer fidelity.

Two reactive ion etching (RIE) steps transfer the pattern first into the chromium hardmask, then into the tungsten layer. The first step uses  $\text{Cl}_2$  and  $\text{O}_2$ . The second step uses  $\text{SF}_6$  and  $\text{O}_2$  at a low 4 mTorr pressure and -35°C substrate temperature.

The final zone plates had a diameter of 200  $\mu\text{m}$ , outermost zone width of 30 nm, and thickness up to 660 nm.

## 2.2 Results

Fabricated zone plates were characterized at the Diamond Light Source at the coherence branchline I13-1. The optics produced a diffraction-limited 36 nm focal spot at the first order using 8.2 keV photon energy. The best efficiency at the same energy was 2.2%.

## 2.3 Usage

The tungsten zone plates were used during the first commissioning experiment at the MAX IV synchrotron radiation facility. The goal was to test the performance of the beamline all the way from the source to the detector. The experiment was a success, showing approx. 50 nm resolution in scanning transmission x-ray microscopy imaging.<sup>3</sup>

## 2.4 Challenges

Process parameters had to be optimized to obtain tungsten films with low internal stress for several reasons. First, minimizing internal stress while depositing tungsten reduces the grain size in the film and increases achievable etch resolution in the material. Second, stress in the film significantly deforms the membrane substrate. Last, if the internal stress is very high, the film can crack or delaminate from the substrate entirely.

The main method to reduce internal stress in tungsten is to introduce nitrogen gas during the tungsten sputtering deposition step. Unfortunately, this can decrease the density of the deposited film<sup>4</sup> and, therefore, reduces the efficiency of the device. Energy-dispersive x-ray spectroscopy studies of our films suggest that the density of the films was only 40–50% of bulk tungsten. We now believe that this was in fact the main contribution to the optics performing below expectations, contrary to the first report stating that it was due to the flawed etching profile.<sup>2</sup> While it is possible to deposit a high density tungsten film, the optimal process pressure window during the sputtering step is extremely small, requiring very precise tuning of the deposition step.

Nevertheless, the fact remains that it is difficult to maintain a vertical sidewall etching profile in patterns with linewidth smaller than 50 nm. Sidewall angles can be controlled by etching at cryogenic temperatures, as

\*Corresponding author: Karolis Parfeniukas [karolisp@kth.se](mailto:karolisp@kth.se), <http://biox.kth.se>

well as low process gas pressure. Unfortunately, process iteration in our case led to being limited by the lowest stable gas pressure in our RIE tool during the tungsten etching step.

In addition, hardmask erosion during RIE leads to ion scattering effects that result in bowing of the tungsten structures, as was shown in the original article.<sup>2</sup> Therefore, more resilient hardmask options should be explored in order to improve the results of this fabrication process.

In summary, given the challenges posed on several fronts in developing the tungsten process further, we opted to pursue an alternative zone plate fabrication method.

### 3. SILICON-BASED ZONE PLATES

In view of the challenges of fabricating hard x-ray zone plates, alternative methods have emerged in recent years. In particular, a new paradigm has been successful: producing high-aspect ratio structures of low-Z materials and using them as a mold for high-density materials. One of these methods structures silicon by metal-assisted chemical etching (MACE) and coats it with platinum by atomic layer deposition (ALD).<sup>5</sup> We have adapted this approach and we present our progress. We outline our fabrication process, observe critical steps, and briefly discuss its potential and limitations.

#### 3.1 Fabrication

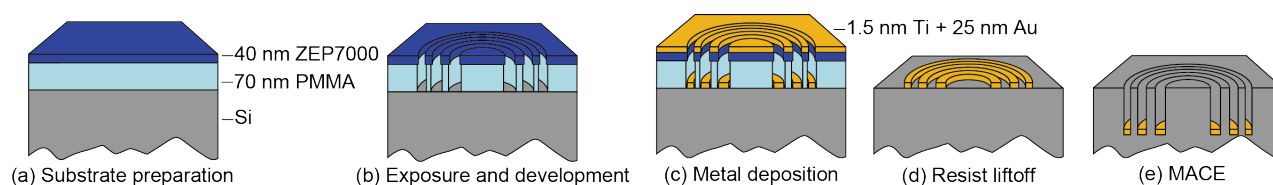


Figure 2. Fabrication process of silicon zone plates. (a) Substrate preparation. (b) The zone plate pattern is written using electron beam lithography and then developed. (c) A gold layer is deposited along with a thin titanium adhesion layer. (d) The resist is stripped, leaving only the necessary gold. (e) The pattern is etched into silicon.

Figure 2 illustrates the fabrication process of silicon zone plates. A bilayer resist stack is prepared on a silicon substrate: 70 nm poly(methyl methacrylate) (PMMA), 40 nm ZEP7000. The sample is baked at 170°C on a hotplate after spinning each resist. The pattern defining the zone plate structures is exposed using electron beam lithography. ZEP7000 is developed in hexylacetate, and PMMA is developed in a solution of methyl isobutyl ketone and isopropanol.

Two metal layers are evaporated onto the sample: a thin 1.5 nm titanium adhesive layer and a 25 nm gold film. Then the lift-off step is performed: the resist is stripped, with only the gold required for the pattern remaining. Metal-assisted chemical etching is done in a solution of hydrogen peroxide and hydrofluoric acid.<sup>6</sup> Relevant etching parameters are reactant concentrations and etching time. The etching solution is rinsed out with deionized water. At this point, the resulting trenches may be filled using electroplating or coated with a heavy metal using atomic layer deposition (ALD).

Prototype zone plates had a diameter up to 200  $\mu\text{m}$ , outermost zone width down to 45 nm, and etching depth down to 6  $\mu\text{m}$  with no obvious limit.

#### 3.2 Critical points

There are several critical points in the silicon zone plate fabrication process. Disregarding them can result in one of several types of failure, ranging from inhibition of the MACE mechanism, to MACE path deviation, to structural collapse of finished structures. The important aspects of the fabrication process and underlying causes of each failure type are outlined in this subsection.

### 3.2.1 Gold adhesion

The gold film has to adhere to the surface of the silicon substrate in order for the MACE reaction to start and continue. Silicon wafers with native oxide do not exhibit good adhesion to gold. Therefore, a titanium adhesion layer was used. To further decrease the chance of gold delamination, a solvent rinsing procedure and an oxygen plasma cleaning step were used to clean the silicon substrates before starting the fabrication process.

### 3.2.2 Lift-off

Typical lift-off process concerns apply when preparing the gold pattern for MACE. The desired gold pattern is only produced if the lift-off step is performed correctly.

In order for the evaporated gold to deposit on the exposed substrate, no resist should be left in the trenches of the structures to block the gold. A short oxygen plasma ashing step was used to ensure that.

If the gold film on the substrate connects with the film on top of the resist, the lift-off step can fail with some undesired gold remaining. This material can either stay in place throughout the entire fabrication process and etch undesired areas, or detach at some point in the fabrication process before the MACE reaction and start it at unexpected places on the chip. This issue typically happens because of the deposited metal film being too thick with respect to the resist.

Finally, the resist pattern should also be transferred to the gold film pattern with no increase of line edge roughness. Assuming the edges of the developed resist are smooth, the deposited film on the substrate should also have low line edge roughness. If there are contact points between the metal layer on the substrate and the layer on the resist, trying to remove the latter can tear away parts of the former. For this reason, the lift-off step should be performed gently. In the case of performing the lift-off step in an ultrasonic bath, it should be done using the lowest power setting.

### 3.2.3 MACE

For the MACE step itself, there are a few possible issues that can influence the rate of the reaction or the etching path.

If there are surface contaminants on the surface before the MACE step, the reaction can be completely inhibited or the reaction rate can be severely reduced. Typical environmental exposure contamination can be eliminated by an oxygen plasma cleaning step.

Then, a sufficiently high reaction rate needs to be maintained by having ample hydrofluoric acid and hydrogen peroxide in the etching solution. A shortage of either reactant will slow down MACE since the principle depends on the presence of both to first oxidize silicon at the catalyst and subsequently etch the forming silica.

Even though the MACE path is expected to follow a straight vertical profile, it has nevertheless been documented that at certain conditions this does not happen. Specifically, electron-hole imbalance has been previously cited.<sup>5,7</sup> During our experiments, two process parameters have been confirmed as having some influence on the directionality of the etching process.

First, the metal film should be uniform. Large grain size or line edge roughness can influence local electron-hole balance and may change the etching path.<sup>7</sup>

And second, the metal film needs to mechanically support itself and be rather rigid. For example, if there are unsupported elongated structures, they can be prone to twisting and bending.<sup>7</sup> These mechanical deformations can be somewhat reduced by making the metal film thicker, but they are eliminated by designing a pattern that is self-supporting. However, fabricating free-standing structures has implications for structure stability, discussed in the next subsection.

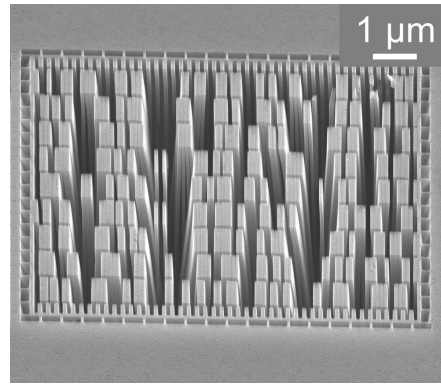


Figure 3. Structure collapse due to capillary forces while drying the sample after MACE. The structures are approx.  $7\ \mu\text{m}$  tall, and their cross-section is  $100\ \text{nm} \times 1\ \mu\text{m}$ .

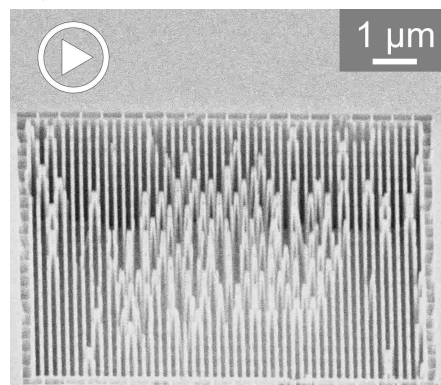


Figure 4. Video 1: pair-wise collapse triggered by SEM imaging. The structures are  $3\ \mu\text{m}$  tall, and their cross-section is  $100\ \text{nm} \times 400\ \text{nm}$ . The recorded video shows real-time structure collapse. <http://dx.doi.org/10.1117/12.2272695.1>

### 3.2.4 Structural integrity

Following the advice from the previous subsection to implement self-supporting gold patterns in the end means unsupported high aspect-ratio silicon structures. They are prone to collapsing due to capillary forces as shown in Fig. 3 but the problem can be avoided by using critical point drying after MACE. Nevertheless, scanning electron microscopy (SEM) imaging can cause charge buildup in free-standing structures that can lead to pair-wise collapse, as demonstrated in Fig. 4. Obviously, structural collapse can be avoided by having integrated supports, but that requires terminated gold patterns that result in problems outlined in the previous section. So far, we have opted to constrain our prototype devices to mechanically stable free-standing silicon structures.

### 3.3 Substrate thinning

The silicon substrate must be thin enough to allow a sufficient amount of x-rays through. In addition, the substrate has to be homogeneous in its thickness in order to preserve the desired phase shift in the zone plate structures. This is a considerable challenge to overcome considering that a natural etch stop cannot be used in the case of a silicon wafer. Nevertheless, we envision two rather straight-forward solutions.

First, silicon can be chemically etched along preferential crystal planes,<sup>8</sup> typically using potassium hydroxide (KOH) or tetramethyl ammonium hydroxide (TMAH). Etching along the  $\langle 100 \rangle$  and  $\langle 110 \rangle$  planes is around 100 times faster than along the  $\langle 111 \rangle$  plane, allowing a pyramid-like structure to be etched into the substrate. Stopping the etch precisely before it etches through the wafer has been identified in our experiments as a possible hurdle for this thinning implementation. Our proposed solution is to monitor the remaining material using infrared or visible light transmission in the etched area and stop the process when the substrate reaches the

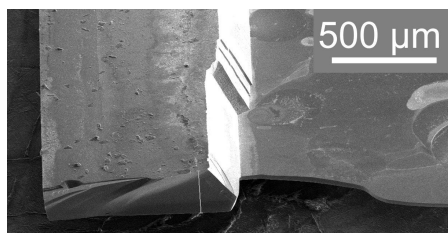


Figure 5. Substrate thinned using potassium hydroxide. A 250  $\mu\text{m}$   $\langle 100 \rangle$  silicon substrate was thinned to sub-20  $\mu\text{m}$ .

desired thickness. In Figure 5 we demonstrate such thinning of a silicon wafer from 250  $\mu\text{m}$  down to sub-20  $\mu\text{m}$  with a mixture of KOH and water. For comparison, the optimal thickness of a silicon zone plate with maximum first-order diffraction efficiency at 8.2 keV photon energy is 10.2  $\mu\text{m}$ . If we fabricated this kind of zone plate in our silicon wafer, it would leave a 9.8  $\mu\text{m}$  silicon substrate with 12% photon absorption. This is an acceptable loss since we expect a much larger increase in overall device efficiency compared to modern high-resolution zone plates due to increased aspect ratio potential.

An alternative method of thinning the substrate is RIE using a mixture of sulfur hexafluoride ( $\text{SF}_6$ ) and oxygen gas. The etching rate can be upwards of 3  $\mu\text{m}/\text{min}$ . Etching anisotropy and slope angles can be controlled with other parameters if needed.<sup>9</sup> The disadvantage of this method is that the etching rate and profile are highly dependent on mask geometry and process parameters. Therefore, uniformity over the entire thinned area can only be achieved by precise RIE parameter tuning.

Independent of the chosen method, care must be taken with regard to the zone plate structures. If the substrate is thinned after the zone plate fabrication, the optic structures have to be protected from the etchant. On the other hand, if the sample is thinned before the zone plate fabrication, the thin silicon membrane must be stable enough to withstand all remaining fabrication steps.

### 3.4 Strategies

Fresnel zone plates can be manufactured using MACE by following one of the following strategies.

The first approach is to use silicon as the phase shifting material. In this case, the gold pattern used for MACE is equivalent to the desired phase shifting structures. As a consequence, the line-to-space ratio in silicon has to be 1:1.

The second approach is to manufacture a silicon zone plate as outlined in the previous paragraph, but fill the gaps in-between the silicon structures with gold or another metal by, e.g., electroplating. Then the structures don't have to be as deep in order to achieve optimal diffraction efficiency. For example, at 8.2 keV photon energy, the maximum first-order diffraction efficiency using gold is achieved with 1.6  $\mu\text{m}$ -thick gratings, while it requires 7.2  $\mu\text{m}$ -thick silicon gratings to achieve the same efficiency. In that case the required aspect ratio is reduced by a factor of 4.5, making fabrication significantly easier.

The third approach is to fabricate so-called frequency-doubled zone plates. Here, a sparse 1:3 line-to-space ratio design is prepared and subsequently coated with a heavy metal. For example, iridium or platinum can be deposited using ALD. We present one such silicon/iridium device in Figure 6. The zone plate is 60  $\mu\text{m}$  in diameter, the outermost zone width is 45 nm, and the feature depth is expected to be around 500 nm.

This strategy also has the advantage of not requiring very high aspect ratios, but at the same time it can reach smaller linewidths with less demands on the lithography due to the sparse 1:3 line structure. On the other hand, ALD can only produce layers of uniform thickness so they can be matched only to a specific portion of the zone plate. Nevertheless, the thicknesses of both the silicon structures and the ALD coating can be tuned towards either efficiency or resolution.<sup>10</sup>

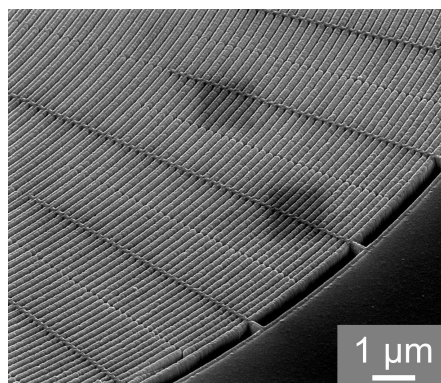


Figure 6. Frequency-doubled iridium zone plate. The 1:3 line-to-space ratio silicon mold was prepared using MACE, and coated with iridium using ALD. The outermost zone width is 45 nm. The dark rectangular areas are SEM imaging artifacts.

### 3.5 Potential and limitations

Practically infinite aspect ratio for zone plate fabrication up to now was available only to multilayer Laue lenses. Their limitation, however, is aperture size, which is not a constraint for MACE fabrication since there is no obvious limit to achievable etching depth. Arbitrarily high aspect ratio can be achieved by designing a pattern that enables uniform MACE and simultaneously provides sufficient support for free-standing silicon structures.

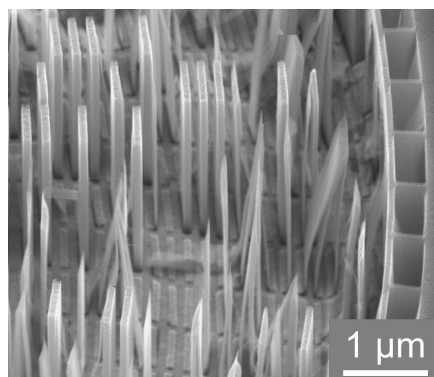


Figure 7. Smallest structure width potential is shown. The gold lift-off process failed by leaving only very thin openings for silicon, but some of the resulting thin structures are still standing even without support. The thinnest observed structures are sub-10 nm.

Structure height can be controlled by tuning the MACE reaction parameters, primarily the reaction time. Structure width is limited only by current lithography and lift-off process capabilities, as can be seen in Figure 7.

Unfortunately, modern zone plate fabrication techniques such as double-sided patterning<sup>11</sup> and interlacing<sup>12</sup> would be difficult to adapt. This is due to the top-down fabrication nature of the MACE process that does not start with a thin, electron-transparent substrate that allows lithographic steps on both sides of the substrate to be aligned with each other. On the other hand, MACE can produce tall, rigid silicon structures for high-efficiency performance that may not require double-sided fabrication methods.

## 4. SUMMARY

Metal-assisted chemical etching is seen as the prime candidate to replace current methods of manufacturing standard Fresnel zone plate optics for hard x-ray nanoimaging. The main reason is the virtually infinite achievable

aspect ratio. Even though we point out several critical points in MACE fabrication, we believe that none of them truly hinder fabrication of zone plates that are simultaneously high-resolution and high-efficiency.

## ACKNOWLEDGMENTS

A portion of this work was carried out with the support of the Diamond Light Source. We thank Diamond Light Source for access to beamline I-13-1 (proposal number MT12046) that contributed to the results presented here. We gratefully acknowledge financial support from the Swedish Research Council (grant ID C0242401) and the Knut and Alice Wallenberg Foundation.

## REFERENCES

- [1] Attwood, D. and Sakdinawat, A., [*X-Rays and Extreme Ultraviolet Radiation: Principles and Applications*], Cambridge University Press (2016).
- [2] Parfeniukas, K., Rahomäki, J., Giakoumidis, S., Seiboth, F., Wittwer, F., Schroer, C. G., and Vogt, U., “Improved tungsten nanofabrication for hard x-ray zone plates,” *Microelectronic Engineering* **152**, 6–9 (2016).
- [3] Vogt, U., Parfeniukas, K., Stankevič, T., Kalbfleisch, S., Matej, Z., Björling, A., Liebi, M., Carbone, G., Mikkelsen, A., and Johansson, U., “First x-ray nanoimaging experiments at NanoMAX,” *Proc. SPIE* **10389** (2017).
- [4] Lee, T., Lee, S., and Ahn, J., “Development of x-ray mask fabrication process using W-sputtering,” *Metals and Materials* **3**(4), 272–276 (1997).
- [5] Chang, C. and Sakdinawat, A., “Ultra-high aspect ratio high-resolution nanofabrication for hard x-ray diffractive optics,” *Nature Communications* **5** (2014).
- [6] Li, X. and Bohn, P. W., “Metal-assisted chemical etching in HF/H<sub>2</sub>O<sub>2</sub> produces porous silicon,” *Applied Physics Letters* **77**(16), 2572 (2000).
- [7] Hildreth, O. J., Lin, W., and Wong, C. P., “Effect of catalyst shape and etchant composition on etching direction in metal-assisted chemical etching of silicon to fabricate 3D nanostructures,” *ACS Nano* **3**(12), 4033–4042 (2009).
- [8] Kendall, D. L., “Vertical etching of silicon at very high aspect ratios,” *Annual Review of Materials Science* **9**(1), 373–403 (1979).
- [9] Liu, Z., Wu, Y., Harteneck, B., and Olynick, D., “Super-selective cryogenic etching for sub-10 nm features,” *Nanotechnology* **24**(1), 015305 (2013).
- [10] Marschall, F., Vila-Comamala, J., Guzenko, V., and David, C., “Systematic efficiency study of line-doubled zone plates,” *Microelectronic Engineering* **177**, 25 – 29 (2017). Advances in Micro- and Nano-Patterning.
- [11] Mohacsi, I., Vartiainen, I., Guizar-Sicairos, M., Karvinen, P., Guzenko, V. A., Müller, E., Färm, E., Ritala, M., Kewish, C. M., Somogyi, A., and David, C., “High resolution double-sided diffractive optics for hard x-ray microscopy,” *Optics Express* **23**(2), 776 (2015).
- [12] Mohacsi, I., Vartiainen, I., Rösner, B., Guizar-Sicairos, M., Guzenko, V. A., McNulty, I., Winarski, R., Holt, M. V., and David, C., “Interlaced zone plate optics for hard x-ray imaging in the 10 nm range,” *Scientific Reports* **170**, 969 (2017).